

Thermal Hall Effect of Spin Excitations in a Kagome Magnet

Max Hirschberger,¹ Robin Chisnell,^{2,*} Young S. Lee,^{2,3} and N. P. Ong¹

¹*Department of Physics, Princeton University, Princeton, New Jersey 08544, USA*

²*Department of Physics, Massachusetts Institute of Technology, Cambridge, Massachusetts 02139, USA*

³*Departments of Applied Physics and Photon Science, Stanford University and SLAC National Accelerator Laboratory, Stanford, California 94305, USA*

(Received 23 June 2015; published 3 September 2015)

At low temperatures, the thermal conductivity of spin excitations in a magnetic insulator can exceed that of phonons. However, because they are charge neutral, the spin waves are not expected to display a thermal Hall effect. However, in the kagome lattice, theory predicts that the Berry curvature leads to a thermal Hall conductivity κ_{xy} . Here we report observation of a large κ_{xy} in the kagome magnet Cu(1-3, bdc) which orders magnetically at 1.8 K. The observed κ_{xy} undergoes a remarkable sign reversal with changes in temperature or magnetic field, associated with sign alternation of the Chern flux between magnon bands. The close correlation between κ_{xy} and κ_{xx} firmly precludes a phonon origin for the thermal Hall effect.

DOI: [10.1103/PhysRevLett.115.106603](https://doi.org/10.1103/PhysRevLett.115.106603)

PACS numbers: 72.10.Di, 72.15.Eb, 72.20.My, 72.25.-b

In a magnetic insulator, experiments on the magnon heat current can potentially yield incisive information on novel quantum magnets. An example is the chiral magnet [1], in which unusual spin textures engender a finite Berry curvature $\Omega(\mathbf{k})$ [$\Omega(\mathbf{k})$ acts like a magnetic field in \mathbf{k} space]. In its presence, a magnon wave packet subject to a potential gradient acquires an anomalous velocity perpendicular to the gradient [2–4]. The most surprising outcome [1,5,6] is that the neutral heat current can be deflected left or right by a physical magnetic field \mathbf{H} as if a Lorentz force were present. The predicted thermal Hall conductivity κ_{xy} was observed in two recent experiments on the ordered magnet $\text{Lu}_2\text{V}_2\text{O}_7$ [7] and the frustrated quantum magnet $\text{Tb}_2\text{Ti}_2\text{O}_7$ [8]. However, to test more incisively the role of $\Omega(\mathbf{k})$ and to exclude a phononic origin [9], we need results that can be compared with microscopic calculations based on $\Omega(\mathbf{k})$. An interesting prediction based on the Chern number sign alternation between magnon bands is the induced sign change in κ_{xy} when either temperature or field is varied. Here we report measurements on the planar kagome magnet Cu(1,3-benzenedicarboxylate) [or Cu(1,3-bdc)] [10–12] which can be compared with calculations on the same material [13]. The close correlation between κ_{xy} and κ_{xx} precludes identifying the former with phonons.

In magnets with strong spin-orbit interaction, competition between the Dzyaloshinskii-Moriya (DM) exchange D and the Heisenberg exchange J can engender canted spin textures with long-range order (LRO). Katsura, Nagaosa, and Lee (KNL) [1] predicted that, in the kagome and pyrochlore lattices, the competition can lead to a state with extensive chirality $\chi = \mathbf{S}_i \cdot \mathbf{S}_j \times \mathbf{S}_k$ (\mathbf{S}_i is the spin at site i) and a large thermal Hall effect. Subsequently, Matsumoto and Murakami (MM) [5,6] amended KNL's calculation

using the gravitational-potential approach [14,15] to relate κ_{xy} directly to the Berry curvature. In the boson representation of the spin Hamiltonian, χ induces a complex “hopping” integral $t = \sqrt{J^2 + D^2} e^{i\phi}$ with $\tan \phi = D/J$ [Fig. 1(a), inset] [1,5,13]. Hence as they hop between sites, the bosons accumulate the phase ϕ , which implies the existence of a vector potential $\mathbf{A}(\mathbf{k})$ permeating \mathbf{k} space. The Berry curvature $\Omega(\mathbf{k}) = \nabla_{\mathbf{k}} \times \mathbf{A}(\mathbf{k})$ imparts an anomalous velocity to magnons, leading to a thermal Hall conductivity κ_{xy} . Each magnon band n contributes a term to κ_{xy} with a sign determined by the integral of $\Omega(\mathbf{k})$ over the Brillouin zone (the Chern number). Recently, Lee, Han, and Lee (LHL) [13] calculated how κ_{xy} undergoes sign changes as the occupancy of the bands changes with T or B .

The kagome magnet Cu(1,3-bdc) is comprised of stacked kagome planes separated by $d = 7.97 \text{ \AA}$ [10–12]. The spin- $\frac{1}{2}$ Cu^{2+} moments interact via an in-plane ferromagnetic exchange $J = 0.6 \text{ meV}$ (details in the Supplemental Material [16]).

As we cool the sample in zero B , the thermal conductivity κ (nearly entirely from phonons) initially rises to a very broad peak at 45 K [Fig. 1(a)]. Below the peak, κ decreases rapidly as the phonons freeze out. Starting near 10 K, the spin contribution κ^s becomes apparent. As shown in Fig. 1(b), this leads to a minimum in κ near T_C (1.85 K) followed by a large peak at $\sim \frac{1}{2}T_C$. Factoring out the entropy, we find that κ/T (red curve) increases rapidly below T_C . This reflects the increased stiffening of the magnon bands as LRO is established. Below 800 mK, the increase in κ/T slows to approach saturation. The open black circles represent the phonon conductivity κ_{ph} deduced from the large- B values of $\kappa_{xx}(T, H)$ (see below). Likewise, κ_{ph}/T is plotted as open red circles. The

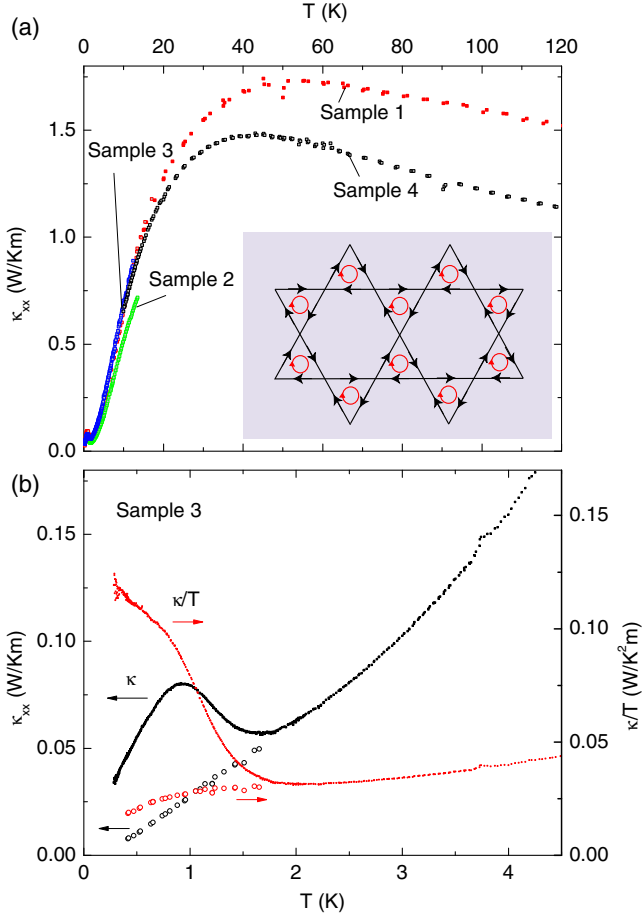


FIG. 1 (color online). The in-plane thermal conductivity κ (in zero B) measured in the kagome magnet Cu(1,3-bdc). At 40–50 K, κ displays a broad peak followed by a steep decrease reflecting the freezing out of phonons [panel (a)]. The spin excitation contribution becomes apparent below 2 K. The inset is a schematic of the kagome lattice with the LRO chiral state [1]. The arrows on the bonds indicate the direction of advancing phase $\phi = \tan^{-1}D/J$. Panel (b) plots κ (black symbols) and κ/T (red) for $T < 4.5$ K. Below the ordering temperature $T_C = 1.8$ K, the magnon contribution to κ appears as a prominent peak that is very B dependent. Values of κ and κ/T at large B (identified with the phonon background) are shown as open symbols.

difference $\kappa - \kappa_{\text{ph}}$ is the estimated thermal conductivity of magnons κ^s in zero B .

Given that Cu(1,3-bdc) is a transparent insulator, it exhibits a surprisingly large thermal Hall conductivity (Fig. 2). Above T_C , the field profile of κ_{xy} is nonmonotonic, showing a positive peak at low B , followed by a zero crossing at higher B [see curve at 2.78 K in Fig. 2(a)]. We refer to a positive κ_{xy} as “ p type.” Below T_C , an interesting change of sign is observed (curves at 1.74 and 0.82 K). The weak hysteresis, implying a coercive field < 1500 Oe at the lowest temperatures, is discussed in the Supplemental

Material [16]. This sign change is investigated in greater detail in sample 3 [we plot κ_{xy}/T in Figs. 2(b) and 2(c)]. The curves of κ_{xy}/T above T_C are similar to those in sample 2. As we cool towards T_C , the peak field H_p decreases rapidly, but remains resolvable below T_C down to 1 K [Fig. 2(c)]. However, as $T \rightarrow 0.6$ K, the p -type response is eventually dominated by an n -type contribution. The thermal Hall response in the limit $B \rightarrow 0$, measured by the quantity $[\kappa_{xy}/BT]_0$ plotted in Fig. 2(d), closely correlates with the growth of κ_s below T_C .

To relate the thermal Hall results to magnons, we next examine the effect of B on the longitudinal thermal conductivity κ_{xx} . As shown in Fig. 3(a), κ_{xx} is initially B independent for $T > 10$ K, suggesting negligible interaction between phonons and the spins. The increasingly strong B dependence observed below 4 K is highlighted in Fig. 3(b). Despite the complicated evolution of the profiles, all the curves share the feature that the B -dependent part is exponentially suppressed at large B , leaving a B -independent “floor” which we identify with $\kappa_{\text{ph}}(T)$ [plotted as open symbols in Fig. 1(b)]. Subtracting the floor allows the thermal conductivity due to spins to be defined as $\kappa_{xx}^s(T, H) \equiv \kappa_{xx}(T, H) - \kappa_{\text{ph}}(T)$. The exponential suppression becomes apparent in the scaled plot of κ_{xx}^s/T vs B/T [Fig. 3(c)]. The asymptotic form at large B in all curves depends only on B/T .

In the interval $0.9 \text{ K} \rightarrow T_C$, κ_{xx}^s displays a V-shaped minimum at $B = 0$ followed by a peak at the field $H_p(T)$. Since κ^s (at $B = 0$) falls rapidly within this interval due to softening of the magnon bands [see Fig. 1(b)], we associate the V-shaped profile with stiffening of the magnon bands by the applied B . At low enough T (< 0.8 K), this stiffening is unimportant and the curves are strictly monotonic. We find that they follow the same universal form. To show this, we multiply each curve by a T -dependent scale factor $s(T)$ and plot them on a semilog scale in Fig. 3(d). In the limit of large B , the universal curve follows the activated form

$$\kappa_{xx}^s \rightarrow T e^{-\beta\Delta}, \quad (1)$$

with the Zeeman gap $\Delta = g\mu_B B$ where $\beta = 1/k_B T$, μ_B is the Bohr magneton, and g the g factor. The inferred value of g (~ 1.6) is consistent with the Zeeman gap measured in a recent neutron scattering experiment.

For comparison, we have also plotted $-\kappa_{xy}/T$ (at 0.47 K) in Fig. 3(d). Within the uncertainty, it also decreases exponentially at large B with a slope close to Δ . Hence, the exponential suppression of the magnon population resulting from Δ is evident in both κ_{xx}^s and κ_{xy} .

LHL [13] have calculated $\kappa_{xy}(T, B)$ applying the Holstein-Primakoff (HP) representation below and above T_C , and Schwinger bosons (SBs) above T_C . In the ordered phase, the HP curves capture the sign changes observed in

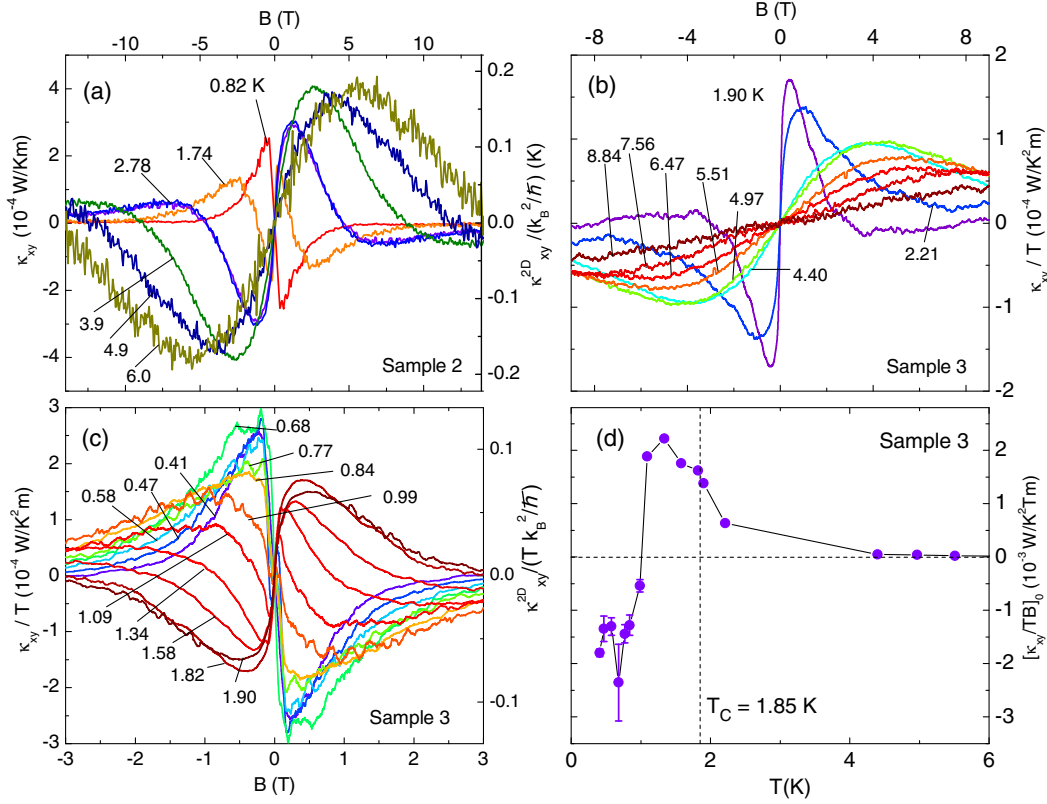


FIG. 2 (color online). The thermal Hall conductivity κ_{xy} measured in Cu(1,3-bdc). In panel (a), we plot the strongly nonmonotonic profiles of κ_{xy} vs B in sample 2. The dispersionlike profile changes sign below ~ 1.7 K. The right scale gives $\kappa^{2D}/(k_B^2/\hbar)$ (per plane) obtained by multiplying κ_{xy} by $d\hbar/k_B^2 = 443.2$ (SI units). Panels (b) and (c) show corresponding curves in sample 3 (now plotted as κ_{xy}/T). Above T_C [panel (b)], κ_{xy}/T is p type. The behavior below 1.90 K is shown in panel (c). At 1.09 K, the n -type contribution appears in weak B , and eventually changes κ_{xy}/T to n -type at all B . Right scale in (c) reports $\kappa_{xy}^{2D}/(Tk_B^2/\hbar)$. In panel (d), we plot the T dependence of the quantity $[\kappa_{xy}/TB]_0$ which measures the thermal Hall response in the limit $B \rightarrow 0$. The T dependence of $[\kappa_{xy}/TB]_0$ closely correlates with κ_{xx}^S vs T (aside from the sign change).

$\kappa_{xy}(T, H)$: a purely n -type curve at the lowest T and, closer to T_C , a sign-change induced by a p -type term. Moreover, the calculated curves at each T exhibit the high-field suppression, in agreement with Fig. 3(d). For sample 3, the peak values of κ_{xy}^{2D} agree with the HP curves (0.04 K at $T = 0.4$ K; 0.2 K at 4.4 K). In the paramagnetic region, however, our field profiles disagree with the SB curves. Above T_C , κ_{xy} is observed to be p -type at all B whereas the SB curves are largely n -type apart from a small window at low B . The comparison suggests that the HP approach is a better predictor than the SB representation even above T_C .

A weak κ_{xy} was reported in Ref. [9] and identified with phonons. A phonon Hall effect based on the Berry curvature was calculated in Refs. [17,18]. Here, however, the evidence is compelling that κ_{xy} arises from spin excitations. The close correlation between the profiles of κ_{xy} and κ_s vs T implies that they come from the same heat carriers. Moreover, the plots in Fig. 3(d) and Eq. (1) show that, when a gap opens, both the longitudinal and Hall

channels are suppressed at the same rate versus B . To us this is firm evidence for spin excitations—the phonon current cannot be switched off by a gap opening in the spin spectrum (we discuss this further in the Supplemental Material [16]).

In addition to confirming the existence of a large κ_{xy} in the kagome magnet, the measured κ_{xy} can be compared with calculations. For chiral magnets, κ_{xy} is capable of probing incisively the effect of the Berry curvature on transport currents.

We acknowledge support from the U.S. National Science Foundation through the MRSEC Grant No. DMR 1420541. N. P. O. was supported by U.S. Army Office of Research (Contract No. W911NF-11-1-0379) and by the Gordon and Betty Moore Foundation's EPIQS Initiative through Grant No. GBMF4539. The work at MIT was supported by the U.S. Department of Energy, Office of Science, Office of Basic Energy Sciences under Grant No. DE-FG02-07ER46134.

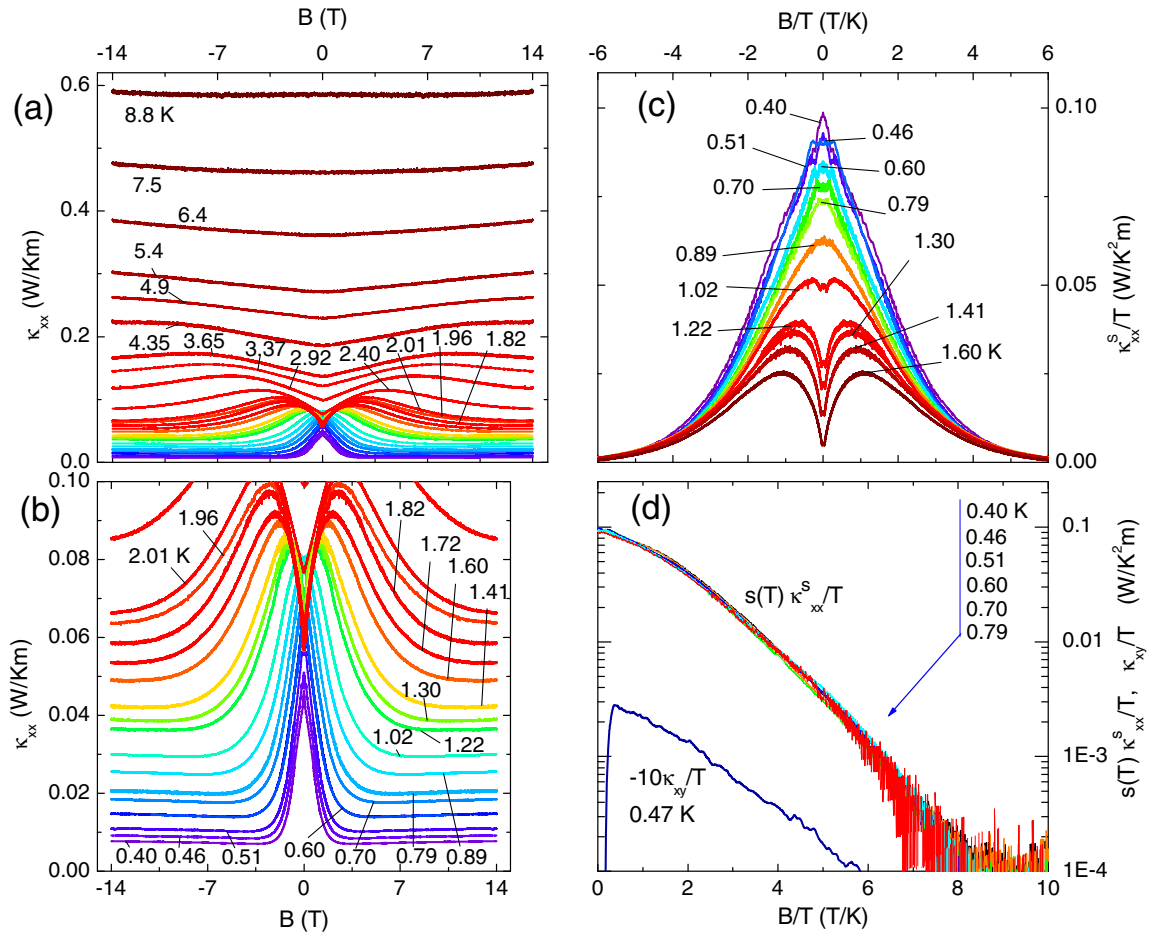


FIG. 3 (color online). The effect of field B on κ_{xx} and scaling behavior at low T , for sample 3. The curves in panel (a) show that the B dependence of κ_{xx} is resolved (in the range $|B| < 14$ T) only at $T < \sim 6.5$ K. The expanded scale in panel (b) shows that, near T_C (1.8 K), κ_{xx} has a nonmonotonic profile with a V-shaped minimum at $B = 0$ (identified with stiffening of the magnon bands by the field). Below 1 K, however, κ_{xx} has a strictly monotonic profile that terminates in a sharp cusp peak as $B \rightarrow 0$. At each $T < T_C$, the constant “floor” profile at large B is identified with κ_{ph} . The pattern in panel (b) simplifies when plotted as κ_{xx}^S/T vs B/T [panel (c)]. Multiplying by a scaling factor $s(T)$ collapses all the curves below 1 K to a “universal” curve, shown on log scale in panel (d). The slope at large B gives a Zeeman gap with $g = 1.6$. The Hall curve $-\kappa_{xy}/T$ has a similar slope at large B .

*Present address: NIST Center for Neutron Research, Gaithersburg, MD 20899, USA.

- [1] H. Katsura, N. Nagaosa, and P.A. Lee, Theory of the Thermal Hall Effect in Quantum Magnets, *Phys. Rev. Lett.* **104**, 066403 (2010).
- [2] D. Xiao, J. Shi, and Q. Niu, Berry Phase Correction to Electron Density of States in Solids, *Phys. Rev. Lett.* **95**, 137204 (2005).
- [3] D. Xiao, M.-C. Chang, and Q. Niu, Berry phase effects on electronic properties, *Rev. Mod. Phys.* **82**, 1959 (2010).
- [4] N. Nagaosa, J. Sinova, S. Onoda, A.H. MacDonald, and N.P. Ong, Anomalous Hall effect, *Rev. Mod. Phys.* **82**, 1539 (2010).
- [5] R. Matsumoto and S. Murakami, Theoretical Prediction of a Rotating Magnon Wave Packet in Ferromagnets, *Phys. Rev. Lett.* **106**, 197202 (2011).
- [6] R. Matsumoto and S. Murakami, Rotational motion of magnons and the thermal Hall effect, *Phys. Rev. B* **84**, 184406 (2011).
- [7] Y. Onose, T. Ideue, H. Katsura, Y. Shiomi, N. Nagaosa, and Y. Tokura, Observation of the magnon Hall effect, *Science* **329**, 297 (2010).
- [8] M. Hirschberger, J.W. Krizan, R.J. Cava, and N.P. Ong, Large thermal Hall conductivity of neutral spin excitations in a frustrated quantum magnet, *Science* **348**, 106 (2015).
- [9] C. Strohm, G.L.J.A. Rikken, and P. Wyder, Phenomenological Evidence for the Phonon Hall Effect, *Phys. Rev. Lett.* **95**, 155901 (2005).
- [10] E.A. Nytko, J.S. Helton, P. Müller, and D.G. Nocera, A structurally perfect $S = \frac{1}{2}$ metal-organic hybrid kagome antiferromagnet, *J. Am. Chem. Soc.* **130**, 2922 (2008).
- [11] L. Marcipar, O. Ofer, A. Keren, E.A. Nytko, D.G. Nocera, Y.S. Lee, J.S. Helton, and C. Bains, Muon-spin spectroscopy of the organometallic spin- $\frac{1}{2}$ kagome-lattice compound Cu(1,3-benzenedicarboxylate), *Phys. Rev. B* **80**, 132402 (2009).

- [12] R. Chisnell, J. S. Helton, D. E. Freedman, D. K. Singh, R. I. Bewley, D. G. Nocera, and Y. S. Lee, Topological magnon bands in a kagome lattice ferromagnet (to be published).
- [13] H. Lee, J. H. Han, and P. A. Lee, Thermal Hall effect of spins in a paramagnet, *Phys. Rev. B* **91**, 125413 (2015).
- [14] J. M. Luttinger, Theory of thermal transport coefficients, *Phys. Rev.* **135**, A1505 (1964).
- [15] H. Oji and P. Streda, Theory of electronic thermal transport—magnetoquantum corrections to the thermal transport-coefficients, *Phys. Rev. B* **31**, 7291 (1985).
- [16] See Supplemental Material at <http://link.aps.org/supplemental/10.1103/PhysRevLett.115.106603> for details on the experimental set up, crystal structure, c-axis thermal conductivity, data from samples 1 and 2, and further discussion of phonon Hall conductivity..
- [17] L. Zhang, J. Ren, J.-S. Wang, and B. Li, Topological Nature of the Phonon Hall Effect, *Phys. Rev. Lett.* **105**, 225901 (2010).
- [18] T. Qin, J. Zhou, and J. Shi, Berry curvature and the phonon Hall effect, *Phys. Rev. B* **86**, 104305 (2012).